Supplementary Information for:

High Power Lithium Ion Micro Batteries from Interdigitated Three-Dimensional Bicontinuous Nanoporous Electrodes

James H. Pikul[1], Hui Gang Zhang[2], Jiung Cho[2], Paul V. Braun[1,2,3,4], and William P. King[1,2,3,4]

[1]*Department of Mechanical Science and Engineering*

[2]*Department of Materials Science and Engineering*

[3]*Frederick Seitz Materials Research Laboratory*

[4]*Beckman Institute for Advanced Science & Technology*

University of Illinois at Urbana – Champaign, IL USA

Email: wpk@illinois.edu

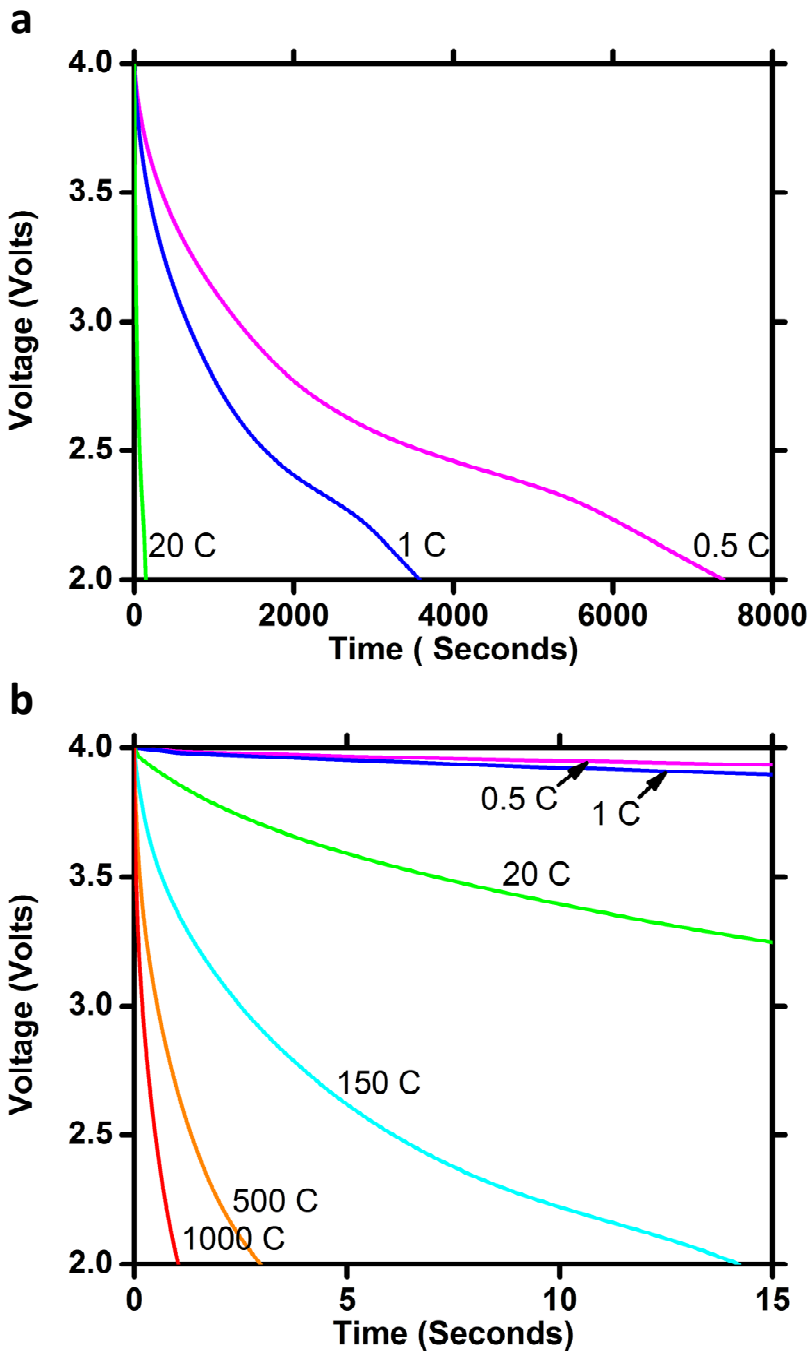

Supplementary Figure S1: Discharge versus time of microbattery H at various C rates. (**b**) Discharge for the first 15 seconds of discharge.

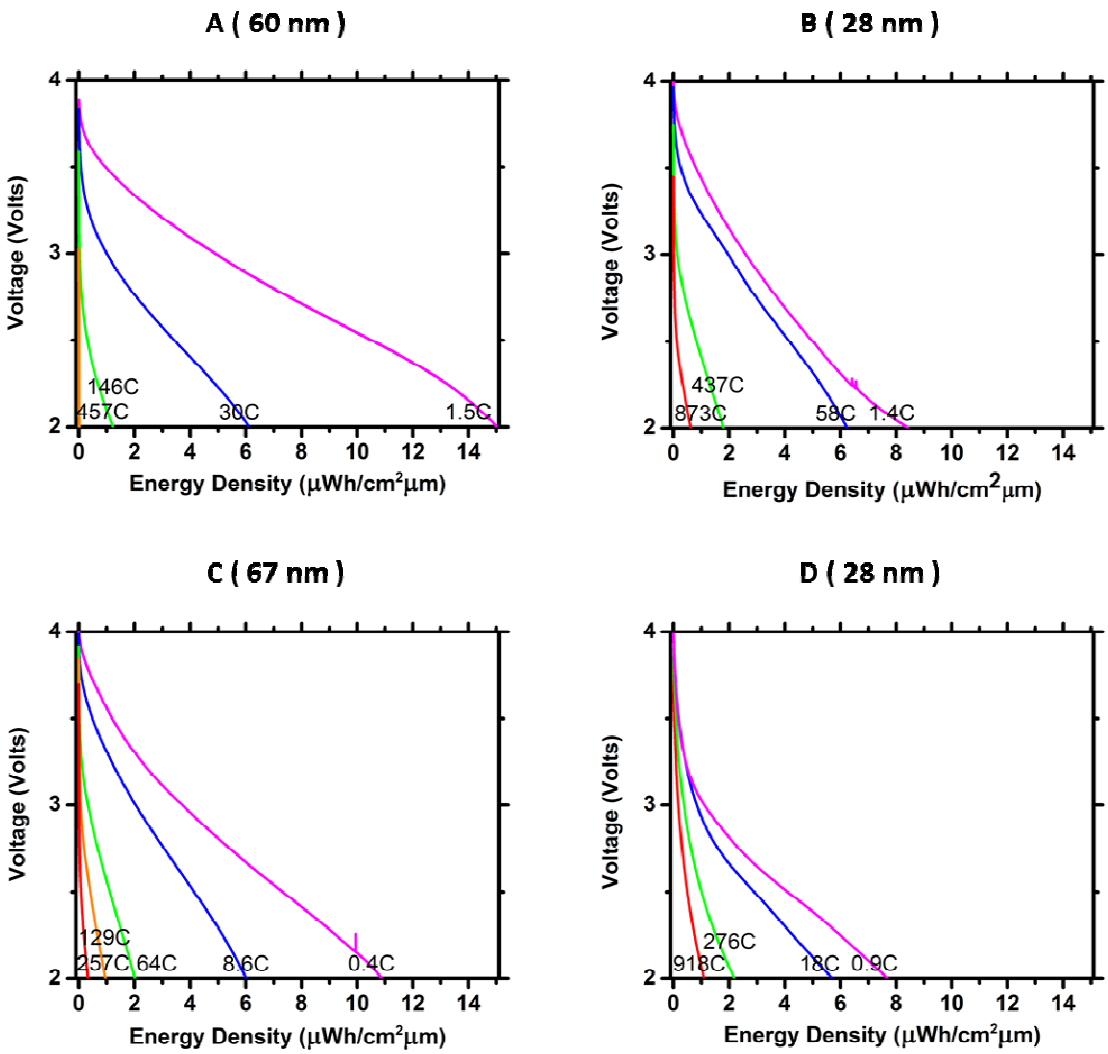
A (60 nm)
B (28 nm)
C (67 nm)
D (28 nm)
Voltage (Volts)
Energy Density (μWh/cm²μm)
146C
457C
30C
1.5C
437C
873C
58C
1.4C
129C
257C
64C
8.6C
0.4C
276C
918C
18C
0.9C

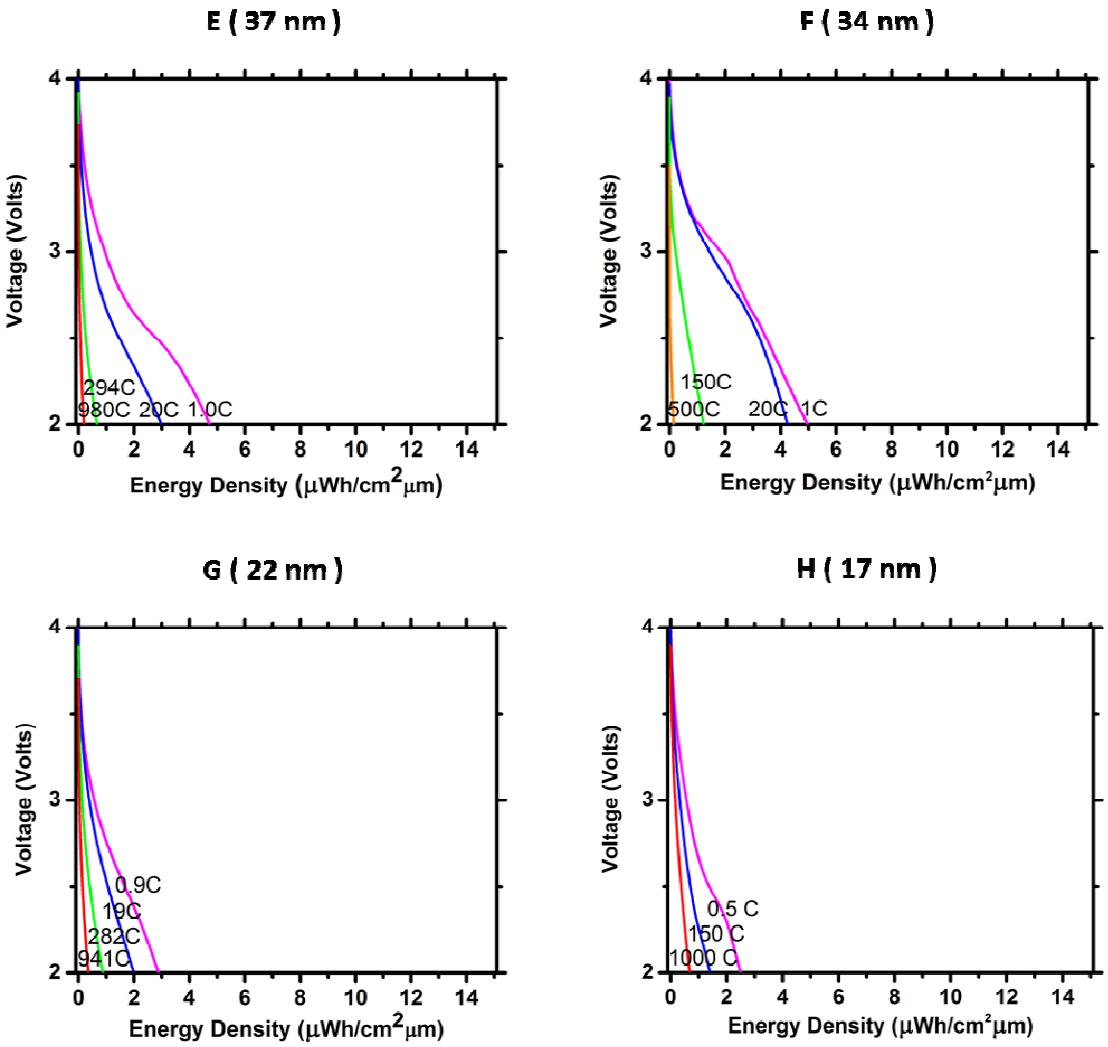

Supplementary Figure S2: Discharge of microbatteries A – H at various C rates. The effective thickness of the cathode active material is labeled in parentheses. The cells were charged galvanostatically at a 1 C current and held at 4.0 volts for 20 minutes between each discharge cycle.

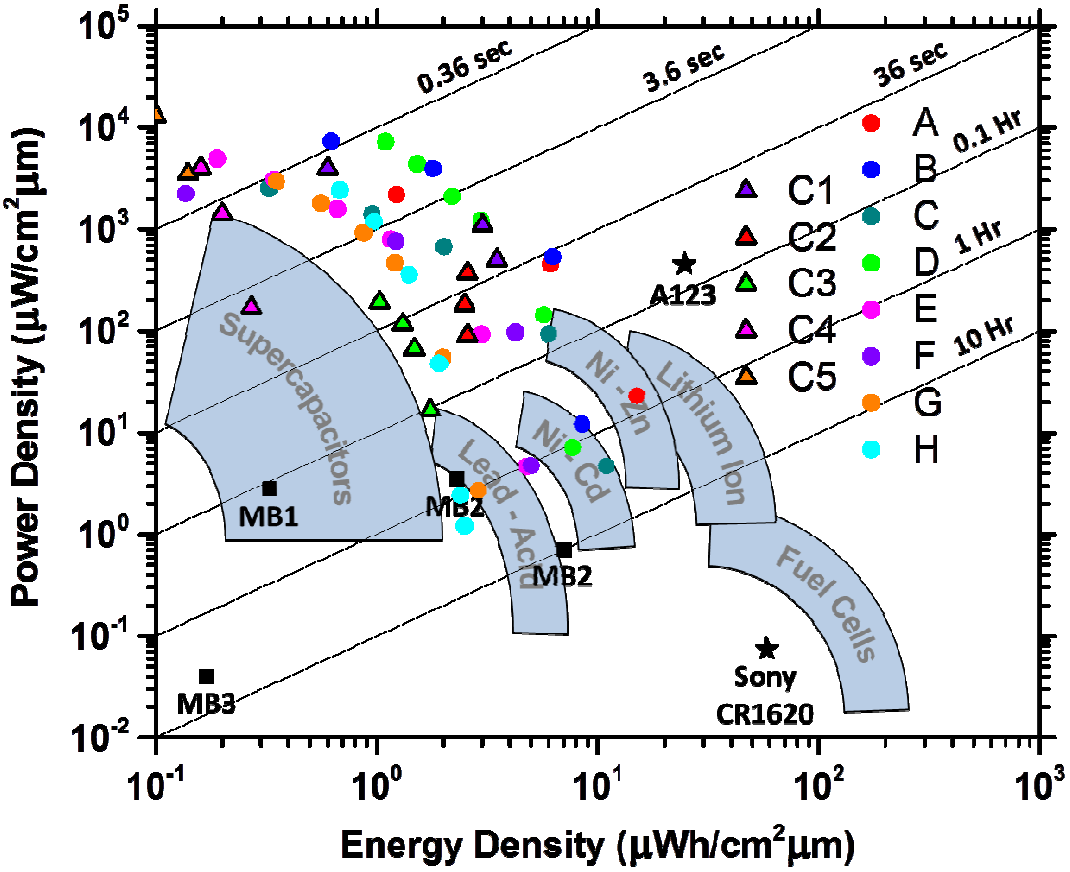

Supplementary Figure S3: Ragone plot showing the performance of our microbatteries and select supercapacitors. The energy and power density of our microbattery cells (A through H) are shown along with high energy density and miniature supercapacitors (C1[4], C2[3], C3[2], C4[26], and C5[4]). The sloping lines on the Ragone plot show the approximate time to remove charge from the device. The plot also shows the performance range of conventional power source technologies, commercial batteries from A123 (high power) and Sony (high energy), and previous microbattery cells having 3D electrodes (MB1 through MB3).

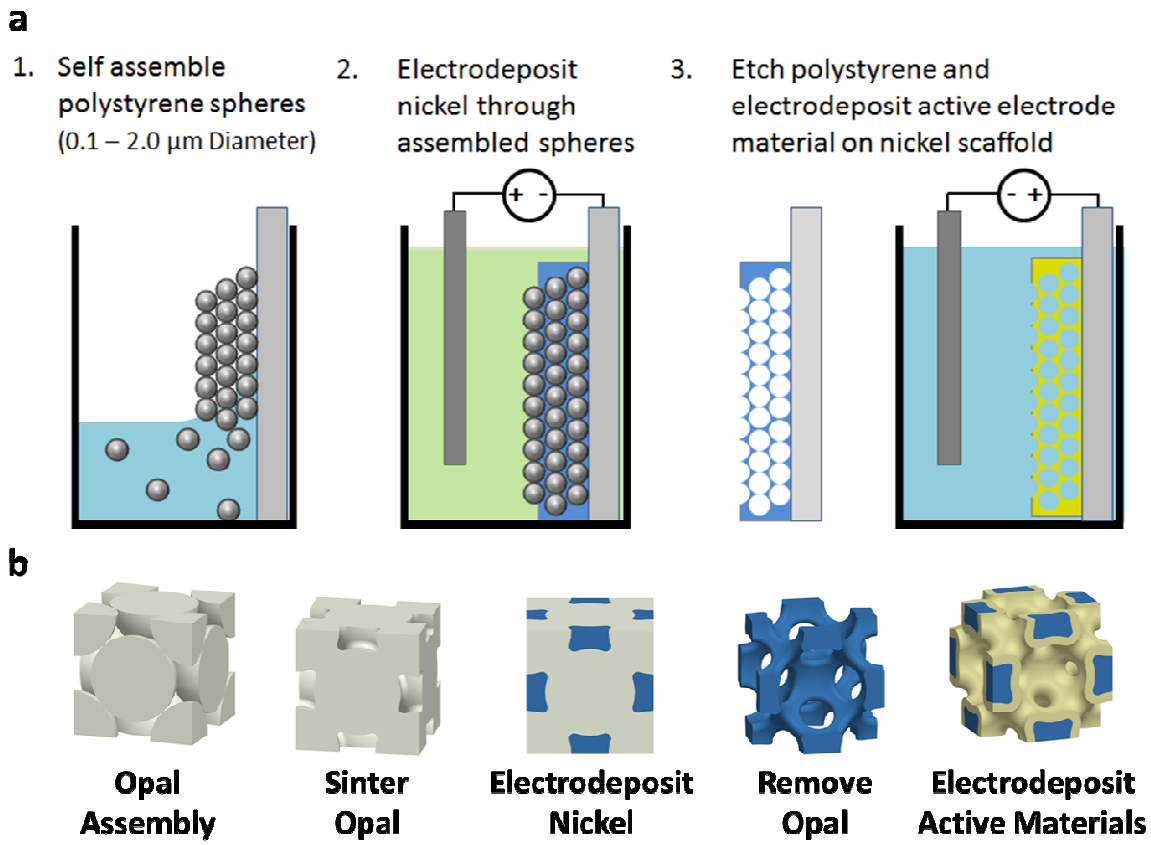

Supplementary Figure S4: Fabrication of the electrodes. (**a**) A substrate with a conductive coating was immersed in a colloid solution of polystyrene spheres in water. During evaporation the spheres self-assembled onto the substrate into an opal assembly, typically face centered cubic in structure. The opal assembly was then sintered at 96 °C. Nickel was then electrodeposited through the voids of the opal assembly using a commercial nickel electroplating solution. After removing the polystyrene with a THF soak and O_2 plasma, the electrolytically active material was electrodeposited onto the nickel using a voltage controlled pulse signal. (**b**) Unit cells of the electrode structure throughout the fabrication process.

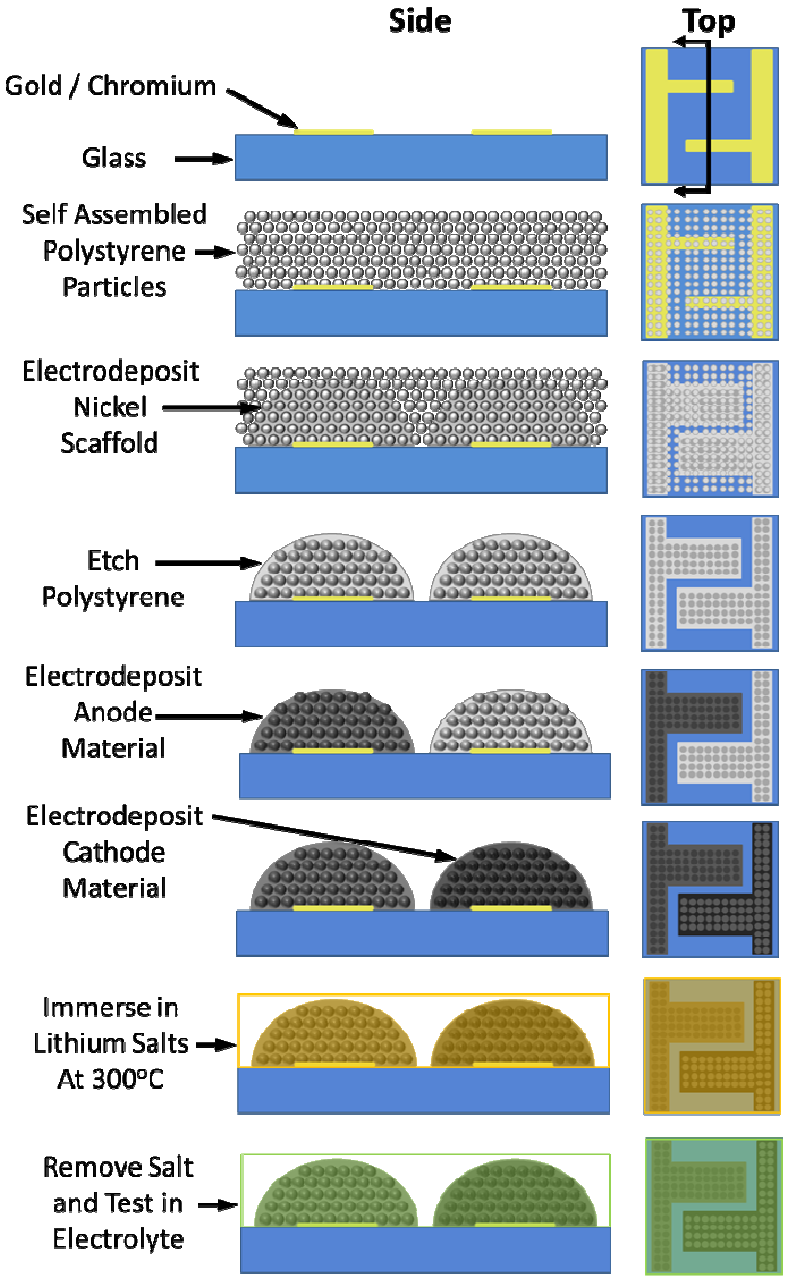

Supplementary Figure S5: Fabrication of the interdigitated microbattery cells. The gold interdigitated electrode template was fabricated onto a 1 mm thick soda lime glass substrate using conventional lithography. The gold was functionalized with a 3-mercapto-1-propanesulfonic acid, sodium salt monolayer after which polystyrene colloids were assembled onto the substrate and the nickel scaffold was electrodeposited. The nickel grew horizontally and vertically during electrodeposition, thus the width of each electrode and the electrode spacing could be precisely controlled by adjusting the nickel deposition time. A nickel – tin alloy was then electrodeposited onto the nickel scaffold corresponding to the anode. MnOOH was then electrodeposited on the nickel scaffold corresponding to the cathode. Finally the substrate was immersed in molten lithium salts, $LiNO_3$ and LiOH, at 300^{o} C to form lithiated manganese oxide.

Supplementary Table S1: Cell geometry and discharge parameters for microbatteries A – H. The thickness of the cathode active material is difficult to measure due to the size, geometry, and porosity of the active material. An effective cathode thickness was approximated for each cell by matching the performance to a diffusion simulation, assuming a constant lithium diffusivity of 2.2 x 10^{-13} cm^2/s. The effective cathode capacity was then calculated using this active material thickness.

Battery	1 C Current (μA)	Footprint (mm^2)	Electrode Height (μm)	Pore Size (nm)	Effective Cathode Thickness (nm)	Effective Cathode Capacity (mAh/g)	Electrode Width (μm)	Electrode Pitch (μm)
A	1.7	2	14.9	500	60	120	33	45
B	0.7	1.7	12.6	500	28	185	28	45
C	0.6	1.5	9.9	500	67	70	22	27
D	1.5	3.5	15.2	500	28	130	40	50
E	0.5	1.9	14.9	500	37	70	33	45
F	0.5	1.8	14.7	330	34	40	38	45
G	0.25	1.6	14.9	500	22	70	33	45
H	0.5	4.6	11.7	330	17	50	30	45

Supplementary Table S2: Volumetric energy and power density at the highest and lowest discharge rates for microbatteries A – H.

Battery	Low Rate		High Rate	
	Energy ($\mu Wh/cm^2\mu m$)	Power ($\mu W/cm^2\mu m$)	Energy ($\mu Wh/cm^2\mu m$)	Power ($\mu W/cm^2\mu m$)
A	15.0	22.9	0.01	5870
B	8.4	12.0	0.62	7360
C	10.9	4.7	0.08	4450
D	7.7	7.1	1.09	7260
E	4.7	4.6	0.19	4900
F	5.0	4.7	0.005	3920
G	2.9	2.7	0.39	2940
H	2.5	1.2	0.68	2420

Supplementary Table S3: Area, finger width, and finger separation for microbattery templates T1 – T3.

Templates	Area (mm x mm)	Finger width (μm)	Finger Separation (μm)
T1	3 x 35	5	40
T2	3 x 35	3	24
T3	5.5 x 35	10	40

Supplementary Note 1: Microbattery comparison to supercapacitors.

Figure S10 compares the volumetric energy and power density of our microbatteries to the energy and power density of some of the most recent and highest performance supercapacitors, including two recently published in *Science*[3,26]. The power densities of the microbatteries are equivalent to or exceed the power densities of most supercapacitors. Microbatteries B and D have higher power density than the power density reported by supercapacitors C1 – C4. The supercapacitors were discharged in the range of 4 to 0 volts, whereas microbatteries A – H output their power over a higher and more consistent range of 4 to 2 volts, which is important when integrating power management electronics with energy storage devices. Supercapacitor C5 has the highest power density of 13 $mW/cm^2\mu m$, but achieves this with the lowest energy density of 0.1 $\mu Wh/cm^2\mu m$. There is a sharp cutoff in the maximum energy density of the supercapacitors, around 4.0 $\mu Wh/cm^2\mu m$. Six of our microbatteries can achieve a higher energy density than 4.0 $\mu Wh/cm^2\mu m$, with the maximum being 15 $\mu Wh/cm^2\mu m$, an almost 4X increase. The energy densities of the microbatteries are initially superior to the supercapcitors, but lose an average 5% total energy density after each cycle. Supercapacitors, however, are known for their ability to achieve up to 10,000 cycles without losing significant energy density[26]. The volumetric energy and power density of supercapacitors C1, C4, and C5 were published and converted to the units used here, as well as adjusted to include the volume of just the electrodes, electrolytes, and separators where needed. The volumetric energy and power density of the active electrode material in supercapacitors C2 and C3 were determined by multiplying the specific energy and power of the carbon electrodes by the density of graphite, assumed 2.23 g/cm^3. The porosity of the electrodes were then determined using the total pore volume per gram of carbon, which was presented in each publication, and the final volumetric

energy and power density was calculated by assuming each device has two electrodes and 10% separator volume.

Supplementary Note 2: Energy storage reactions.

The cathode half-reaction:

$$LiMnO_2 = Li_{1-n}MnO_2 + nLi^+ + ne^-$$

The anode half-reaction:

$$nLi^+ + ne^- + NiSn = Li_yNiSn$$

Supplementary Method

Electrochemical plating solution and deposition properties.

Below are the compositions of the active material plating solutions and the voltage profiles used to deposit the active material onto the 3D nickel scaffold.

MnOOH electrochemical deposition solution:

0.1 M manganese acetate tetrahydrate and 0.1 M sodium sulfate in Milli-Q water.

MnOOH pulsed voltage deposition profile:

1. Surface Preparation

    1.8 volts on for 0.15 seconds, 0 volts off for 4 seconds, cycled 60 – 80 times

2. Deposition

    1.8 volts on for 0.15 seconds, 1.1 volts off for 4 seconds, cycled 40 – 300 times

Ni-Sn electrochemical deposition solution:

100 ml Milli-Q water, 30 g $K_4P_2O_7$, 0.8 g $NiCl_2$, 0.8 g glycine, 0.8 g potassium sodium tartrate, 2.0 g $SnCl_2{\cdot}2H_2O$.

Ni-Sn pulsed voltage deposition profile:

-0.22 volts on for 0.6 seconds, 0 volts off for 3 seconds, cycled 15 – 30 times

References

26. El-Kady M. F., Strong V., Dubin S., Kaner R. B. Laser scribing of high-performance and flexible graphene-based electrochemical capacitors. *Science* **335**, 1326-1330 (2012).